

# Templeting of Thin Films Induced by Dewetting on Patterned Surfaces

Kajari Kargupta and Ashutosh Sharma\*\*

*Department of Chemical Engineering, Indian Institute of Technology, Kanpur, UP 208 016, India*

(Dated: March 22, 2022)

The instability, dynamics and morphological transitions of patterns in thin liquid films on periodic striped surfaces (consisting of alternating less and more wettable stripes) are investigated based on 3-D nonlinear simulations that account for the inter-site hydrodynamic and surface-energetic interactions. The film breakup is suppressed on some potentially destabilizing nonwettable sites when their spacing is below a characteristic lengthscale of the instability ( $\lambda_h$ ), the upper bound for which is close to the spinodal lengthscale. The thin film pattern replicates the substrate surface energy pattern closely only when, (a) the periodicity of substrate pattern matches closely with the  $\lambda_h$ , and (b) the stripe-width is within a range bounded by a lower critical length, below which no heterogeneous rupture occurs, and an upper transition length above which complex morphological features bearing little resemblance to the substrate pattern are formed.

PACS numbers: 68.15.+e, 47.20.Ma, 47.54.+r, 68.08.De, 68.08.Bc

Self-organization during dewetting of thin films on deliberately tailored chemically heterogeneous substrates is of increasing promise for engineering of desired nano- and micro-patterns in thin films by templeting[1, 2, 3, 4, 5, 6, 7, 8, 9, 10, 11]. On a chemically heterogeneous substrate, dewetting is driven by the spatial gradient of micro-scale wettability [12], rather than by the non-wettability of the substrate itself. The latter occurs in the so called spinodal dewetting on homogeneous surfaces [13, 14]. While the rupture of a thin film on a single heterogeneous patch is now well understood, patterned substrates pack a large density of surface features that are closely spaced. How does hydrodynamic interactions between the neighboring heterogeneities affect the pattern evolution dynamics and morphology in thin films? This question, which is addressed here, is central to our understanding of how faithfully the substrate patterns are reproduced in a thin film spontaneously, *i.e.*, how effective is the templeting of soft materials by dewetting route and what are the conditions for ideal templeting? An associated question for both the patterned and naturally occurring heterogeneous surfaces is whether all the potentially dewetting sites remain active or “live” in producing rupture when they are in close proximity. These questions are resolved based on 3-D nonlinear simulations of the stability, dynamics and morphology of thin films on periodic chemically heterogeneous surfaces.

The substrate considered consists of alternating less wettable and more wettable (or completely wettable) stripes that differ in their interactions with the overlying film. The key parameters of the substrate pattern are its periodicity interval (center-to-center distance between two consecutive stripes,  $L_p$ ) and the length-scale of the less wettable stripe (stripe-width,  $W$ ). The following nondimensional thin film equation governs the stability and spatio-temporal evolution of a thin film system subjected to the excess intermolecular interactions [12].

$$\partial H/\partial T + \nabla \cdot [H^3 \nabla (\nabla^2 H)] - \nabla \cdot [H^3 \nabla \Phi] = 0 \quad (1)$$

$H(X,Y,T)$  is non-dimensional local film thickness scaled with the mean thickness  $h_o$ ;  $\Phi = [2\pi h_o^2/|A_s|][\partial \Delta G/\partial H]$ ;  $\Delta G$  is the excess intermolecular interaction energy per unit area and  $A_s$  is the effective Hamaker constant for van der Waals interaction;  $X, Y$  are the non-dimensional coordinates in the plane of the substrate, scaled with a lengthscale  $(2\pi\gamma/|A_s|)^{1/2}h_o^2$ ; and the non-dimensional time  $T$  is scaled with  $12\pi^2\mu\gamma h_o^5/A_s^2$ ;  $\gamma$  and  $\mu$  refer to the film surface tension and viscosity, respectively. The lengthscale of the spinodal instability on a uniform surface is given by,  $\lambda = (-4\pi^2\gamma/(\partial^2 \Delta G/\partial h^2))^{1/2}$ . On a chemically heterogeneous striped surface,  $\Phi = \Phi(H, X, Y)$ . At a constant film thickness, we model the variation of  $\Phi$  in  $X$  direction by a periodic step function of periodicity,  $L_p$ . Gradient of force  $\nabla \Phi$ , at the boundary of the stripes causes flow from the less wettable (higher pressure) stripes to the more wettable (lower pressure) stripes, even when the spinodal stability condition  $\partial \Phi/\partial H > 0$  is satisfied everywhere [12]. It is known that a single stripe in the absence of its neighbors can cause rupture only if its width exceeds a critical lengthscale,  $W_c \ll \lambda$  [12].

We consider general representation of antagonistic (attractive/repulsive) long range and short range intermolecular interactions applicable to the aqueous films (eq. 2) [14, 15] and polymer films on high energy surfaces like silicon (eq. 3) [4, 12, 16]. In both the cases the long range van der Waals force is stabilizing and thus films thinner (thicker) than a critical thickness are unstable (metastable).

$$\Delta G = -(A_s/12\pi h^2) + S_p \exp(-h/l_p) \quad (2)$$

This potential represents aqueous films when the effective Hamaker constant,  $A_s$  and  $S_p$  are both negative (long-range van der Waals repulsion combined with shorter-range attraction, e.g. hydrophobic attraction)[17]. On the hydrophobic stripes ( $A_s^h = -1.41 \times 10^{-20}$  J,  $S_p^h = -65$  mJ/m<sup>2</sup> and  $l_p = 0.6$  nm), the film is spinodally

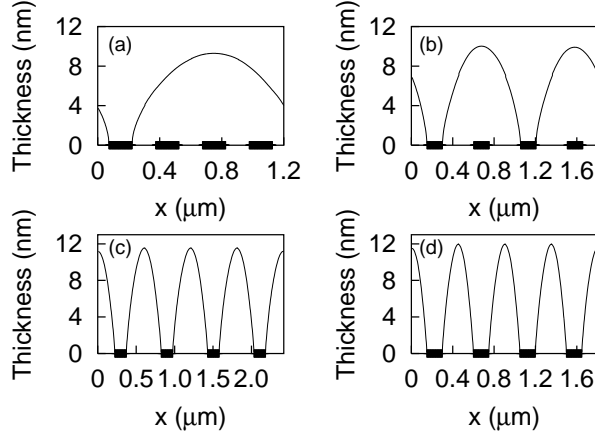


FIG. 1: Equilibrium thin film profile on a striped surface ( $W = 0.16\lambda$ ). The less-wettable stripes are denoted by black rectangles. Figs 1a, 1b and 1c is for a 6nm film for increasing periodicity. Fig 1d shows the profile for a 5.5 nm thin film on a same substrate shown in Fig. 1b.

unstable ( $\partial\Phi/\partial H < 0$ ) below a critical thickness,  $h_c$  of 7.4 nm. The equilibrium contact angle obtained from extended Young-Dupre equation,  $\cos\theta = 1 + \Delta G(h_e)/\gamma$  is  $61^\circ$ ; where  $h_e$  is the equilibrium thickness. On the hydrophilic stripes ( $A_s = -1.41 \times 10^{-20}$  J,  $S_p = -0.61$  mJ/m<sup>2</sup> and  $l_p = 0.6$  nm), the film of any thickness is spinodally stable ( $\partial\Phi/\partial H > 0$ ) and completely wets the surface.

Equation (1) was numerically solved using a central difference scheme in space combined with Gears algorithm for stiff equations for time marching and periodic boundary condition. The critical length,  $W_c$  of a single heterogeneity (hydrophobic patch) that engenders rupture on a large hydrophilic substrate in this case is  $0.08\lambda$ .

Ideal templating requires that dewetting should occur on every less wettable site on the patterned substrate. Fig. 1a shows a single rupture on a substrate containing four potentially dewetting sites ( $n_S = 4$ ) when the periodicity interval is small,  $L_p = 0.45\lambda$ . The resulting lone drop spans across the remaining “inactive” hydrophobic sites. Fig 1a to 1c show increased number of dewetted stripes ( $n_D = 1, 2, 4$ ) and resulting liquid domains as  $L_p$  is increased from  $0.45\lambda \rightarrow 0.68\lambda \rightarrow 0.9\lambda$ . This, as well as a large number of simulations not displayed here showed that on a substrate containing many potentially destabilizing sites, only the sites (randomly picked) separated by a characteristic length-scale of the instability,  $\lambda_h$ , of the order of the spinodal scale,  $\lambda$  remain “live” or effective in causing the film rupture. Dewetting on the remaining intervening sites is suppressed since rupture on each site would require surface deformations on smaller scales resulting in high surface energy penalty. The ratio of this characteristic lengthscale,  $\lambda_h$ , to the spinodal length scale,  $\lambda$ , obtained from simulations, decreases as the potential difference across the stripe boundary, ( $\Delta\Phi$ ) increases (Fig. 2),

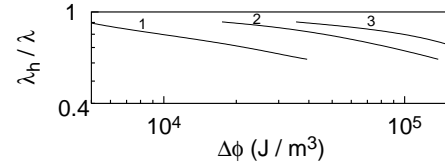


FIG. 2: Variation of the ratio of characteristic to spinodal length scale with potential difference  $\Delta\phi$ , introduced by changing the  $S_p$  of the more wettable stripes.  $-\partial\phi/\partial h$ , for curves 1 ( $h_o = 6$ nm,  $S_p^h = -65$ mJ/m<sup>2</sup>), 2 ( $h_o = 4.5$ nm,  $S_p^h = -19.5$ mJ/m<sup>2</sup>) and 3 ( $h_o = 4.5$ nm,  $S_p^h = -39$ mJ/m<sup>2</sup>) are  $6.47 \times 10^{12}$ ,  $2.4 \times 10^{13}$  and  $5.4 \times 10^{13}$  J/m<sup>4</sup>, respectively.

where  $\Delta\Phi = (\Phi^h - \Phi)$ , evaluated at the initial thickness. For a large value of spinodal parameter (e.g. for thinner films), the ratio approaches very close to 1 unless  $\Delta\Phi$  is very large (curves 2 and 3 of Fig. 2). A simple scale analysis ( $H = 1 + \epsilon$ ,  $\nabla^2\Phi \sim \Delta\Phi/cL^2$ ,  $c < 1$ ), of Eq. (1) [12] leads to the following characteristic lengthscale for growth of instability:  $\lambda_h \propto [\Delta\Phi/\epsilon c - \partial\Phi/\partial H]^{-0.5}$ . Thus the ratio of heterogeneous to spinodal lengthscale,  $\lambda_h/\lambda \propto (1 + \Delta\Phi/(-\epsilon c \partial\Phi/\partial H))^{-0.5}$ ; and  $\lambda_h \sim \lambda$  when spinodal term  $-\partial\Phi/\partial H$  is very strong compared to the applied potential difference. For very large potential difference,  $\lambda_h/\lambda \propto (\Delta\phi)^{-0.5}$ . Thus the upper limit of the characteristic lengthscale of the instability is always bound by the spinodal length,  $\lambda$ . An interesting implication is that even when the rupture occurs by the heterogeneous mechanism on a substrate containing a large density of heterogeneities, the lengthscale of the resulting pattern can give the illusion of spinodal dewetting by mimicking the characteristic lengthscale of the latter. Differentiating true spinodal dewetting from heterogeneous dewetting therefore requires a careful consideration of their distinct time scales and morphological features[12]. Further, the contact line always remains pinned at the boundary of the stripes whenever alternate stripes are completely wettable (Figures 1a – 1d).

Decreased mean film thickness increases both the terms,  $\Delta\Phi$  and  $-\partial\Phi/\partial h$  and thus decreases  $\lambda_h$  non-linearly. Thus, a greater number of nonwettable heterogeneities become active in causing the film breakup for thinner films. Comparison of figs. 1b (thickness = 6 nm,  $\lambda = 0.67$  μm) and 1d (thickness = 5.5 nm,  $\lambda = 0.42$  μm) clearly shows this for an identical substrate pattern. This transition uncovered based on dynamical simulations is also in conformity with the earlier equilibrium energy considerations [1] that are related however only to the equilibrium structures.

From the above discussion, a necessary condition for good templating is that  $L_p \sim \lambda_h (< \lambda)$  which ensures dewetting on every less wettable site ( $n_D = n_S$ ). The condition  $L_p \sim \lambda_h$ , for  $n_D = n_S$ , also remains valid when both the stripes are nonwettable. However, in this case the contact line can move across the boundary of the stripes to the more wettable part. We simulated the 3D morphologies during the evolution of a polymer like film on an oxide (low-energy) covered silicon (high-

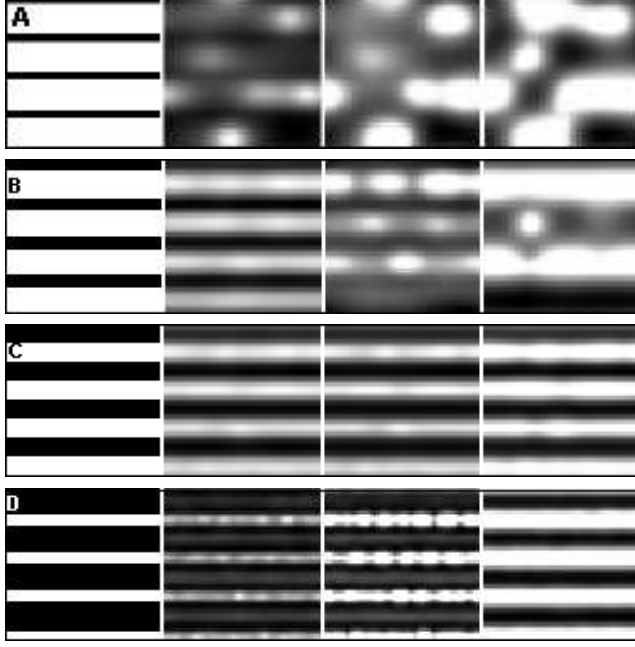


FIG. 3: Morphological evolution in a 5 nm thick film on a striped surface ( $W = 0.8 \mu\text{m} = 0.53 \lambda$ ). In Figures 3A to 3D periodicity of surface pattern,  $L_p$  are  $1 \mu\text{m}$ ,  $1.2 \mu\text{m}$ ,  $1.45 \mu\text{m}$  and  $3 \mu\text{m}$  respectively. The first image in this figure as well as in the subsequent figures represents the substrate surface energy pattern; black and white represent the more wettable part and less wettable part respectively. For other images describing the film morphology, a continuous linear gray scale between the minimum and the maximum thickness in each picture has been used.

energy) substrate. An analytical representation of combined antagonistic (attractive/repulsive) long and short-range intermolecular interactions for a polymer-like film on a coated (e.g. oxide covered) substrate is [12]:

$$-12\pi\Delta G = [(A_s - A_{c1})/(h + d_{c1} + d_{c2})^2 + (A_{c1} - A_{c2})/(h + d_{c2})^2 + A_{c2}/h^2] \quad (3)$$

Negative value of the effective Hamaker constant on the substrate [ $A_s = A_s^h = -1.88 \times 10^{-20}$  J] signifies a long-range repulsion, whereas a positive value on coating [ $A_{c1} = A_{c1}^h = 1.13 \times 10^{-20}$  J] represents an intermediate-range attraction [12]. The non-wettable coating (e.g. oxide) thickness [ $d_{c1} = 2.5$  nm,  $d_{c1}^h = 4$  nm] is increased on alternating stripes which causes the macroscopic contact angle to increase from  $0.58^\circ$  on the more wettable stripes to  $1.7^\circ$  on the less wettable stripes. A still shorter-range repulsion may arise due to chemically adsorbed or grafted layer of the polymer ( $A_{c2} = -0.188 \times 10^{-20}$  J,  $d_{c2} = 1$  nm are the film Hamaker constant and the thickness of the adsorbed layer, respectively) [12]. The representation, eq.[3], is chosen for illustration without affecting the underlying physics, which we have verified for many different potentials.

Figures 3A – 3D depict the effect of periodicity interval,  $L_p$  on the self-organization of a 5 nm thin film

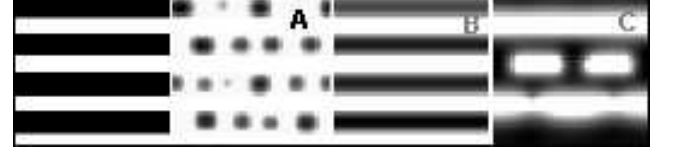


FIG. 4: 3D morphologies at late stages of evolution for films of thickness (A) 2.5 nm, (B) 6.9 nm and (C) 8 nm on a striped surface with  $W = 1.2 \mu\text{m}$  and  $L_p = 3 \mu\text{m}$ .

that is spinodally unstable on both type of stripes. In each case, the evolution starts with local depressions on the less-wettable stripes (Figs. 3A – 3D). For  $L_p$  sufficiently smaller than  $\lambda$  ( $L_p = 1 \mu\text{m}$ ,  $\lambda = 1.51 \mu\text{m}$  based on  $\gamma = 38 \text{ mJ/m}^2$  and  $\mu = 1 \text{ kg/m.s}$ ), the isolated holes or depressions that form along the less wettable stripes grow onto the more wettable regions and coalesce with each other rapidly (Fig. 3A) leading to a disordered structure and very poor templating. Increasing periodicity ( $L_p = 1.2 \mu\text{m}$ ; Fig. 3B) leads to more ordered dewetting, but the number of dewetted regions remain less than the number of less wettable stripes, and defects evolve at late times (e.g., holes in the liquid ridge; image 4 of fig. 3B). For  $L_p \geq \lambda$  (Figures 3C and 3D), the number of dewetted stripes equal the number of less wettable stripes. However, templating in the form of liquid ridges with straight edges is best at an intermediate periodicity,  $L_p \sim \lambda_h (< \lambda)$  (Fig. 3C). A further increase in  $L_p$  makes the width of dewetted region bigger than the width of the less wettable stripe (image 4 of Fig. 3D), i.e., the contact line resides in the interior of the more wettable stripe, rather than close to the boundary.

The transition of surface morphology can also be clearly understood from Fig. 4, which shows that ideal templating occurs for an intermediate thickness (3rd image of Fig. 4) for which the spinodal wavelength,  $\lambda (= 3 \mu\text{m})$  is equal to  $L_p$ . Thinner films evolve by the formation of droplets on the more wettable stripes due to the spinodal mechanism assisted by the Rayleigh instability. For thicker films ( $\lambda > L_p$ ), dewetting occurs on fewer stripes with the formation of holes in broad liquid ridges (e.g., last image of Fig.4).

We found that besides  $L_p$ , the other parameter that governs the thin film pattern is the stripe-width ( $W$ ). It is already known that for a single heterogeneity on a large substrate, increase in the width of the heterogeneity shifts the onset of dewetting from the center of the heterogeneity to the boundary of the heterogeneity [12]. Figs. 5A – 5D shows the transition of patterning with the increase of the stripe-width ( $W$ ), keeping the periodicity,  $L_p$  fixed ( $> \lambda$ ). For small stripe-width ( $\sim 0.4\lambda$ ; Fig. 5A), rupture is initiated at the center of less wettable stripes by the formation of depressions that coalesce to form rectangular dewetted regions of widths greater than the stripe-width. For a larger stripe-width ( $W \sim 0.8\lambda$ ), dewetting is initiated by a layer of holes at each of the

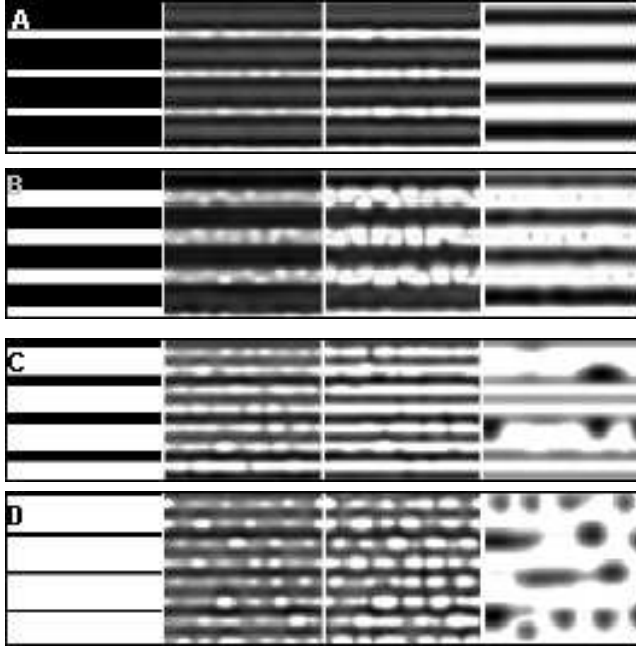


FIG. 5: Morphological evolution in a 5 nm thick film on a striped surface ( $L_p = 3 \mu\text{m} \sim 2\lambda$ ).  $W = 0.6 \mu\text{m}$ ,  $1.2 \mu\text{m}$ ,  $2.1 \mu\text{m}$  and  $2.7 \mu\text{m}$ , respectively for figures 5A – 5D.

two boundaries of the stripe (image 2 of Fig. 5B). Coalescence of these two layers of holes leads to the dewetted regions containing some residual droplets (image 4 of Fig. 5B). Further increase in the stripe width leads to the formation of two layers of holes on each stripe separated by an elevated liquid cylinder (image 2 of Fig. 5C). Thus, at an intermediate stage of evolution, the number of cylindrical liquid ridges becomes twice of the number of more wettable stripes on the substrate (image 3 of Fig. 5C). Eventually, liquid ridges on the less wettable region disintegrate into droplets (not shown). Laplace pressure gradients cause ripening of the structure leading to the merging of droplets with the liquid ridges (image 4 of Fig. 5C). Further increase in the stripe-width breaks the whole order of the substrate pattern due to the formation and repeated coalescence of several layers of holes on each stripe that eventually evolve into arrays of irregular droplets. Thus, a good synchronization of the thin film morphology with the substrate pattern requires an upper limit on the stripe-width ( $W_t \sim < 0.8\lambda$ , for this case). Based on a large number of simulations for different film thickness and for different systems, we have verified that a breakdown of templating due to the off-center dewetting occurs at stripe-widths in excess of about  $0.7\lambda - 0.8\lambda$ .

In conclusion, the 3-D thin film morphology on a patterned substrate during dewetting can be modulated profoundly by a competition among the time scales (spinodal and heterogeneous) and length scales (spinodal, stripe-width, periodicity, thickness) of the problem. On a striped substrate, ideal templating in the form of cylin-

drical liquid ridges covering the more wettable stripes occurs when (e.g., image 4 in fig. 3C): (a) periodicity of the substrate pattern is very close to the characteristic lengthscale,  $\lambda_h$ , and (b) the stripe width is larger than a critical width,  $W_c$ , which is effective in causing rupture by the heterogeneous mechanism, but smaller than a transition width ( $W_t \sim 0.7\lambda - 0.8\lambda$ ), that ensures initiation of dewetting at the stripe-center. Even a very weak wettability contrast (e.g. Fig.3) is sufficient to align the thin film pattern with the template under the above conditions. Predictions of our simulations show close resemblance to the recently reported experimental observations on dewetting of polymers on patterned surfaces that reveal: (a) best templating for an intermediate thickness film [6, 10] and (b) correspondence between the natural length scale and periodicity of the substrate pattern for good templating [4, 5, 6]. Finally, on a completely wettable substrate containing many potentially destabilizing sites, only the sites (randomly picked) separated by a characteristic lengthscale (of the order of the spinodal scale),  $\lambda_h$  remain “live” or effective in causing the film rupture. It is hoped that this study will help in the design and interpretation, creation and rational manipulation of self organized microstructures in thin films by templating.

Discussions with G. Reiter are gratefully acknowledged.

---

\* ashutos@iitk.ac.in

- [1] P. Lenz and R. Lipowsky, Phys. Rev. Lett. **80**, 1920 (1998); P. Lenz and R. Lipowsky, Eur. Phys. J. E. **1**, 249 (2000); R. Lipowsky, P. Lenz and P. S. Swain, Colloid and Surfaces A **161**, 3 (2000).
- [2] H. Gau *et al.*, Science **283**, 46(1999).
- [3] A. Kumar and G. M. Whitesides, Science **263**, 60 (1994).
- [4] L. Rockford *et al.*, Phys. Rev. Lett. **82**, 2602 (1999).
- [5] M. Boltau *et al.*, Nature **391**, 877 (1998).
- [6] M. Nisato *et al.*, Macromolecules **32**, 2356 (1999).
- [7] M. Gleiche, L. F. Chi and H. Fuchs, Nature **403**, 173 (2000).
- [8] D. E. Kataoka and S. M. Troian, Nature **402**, 794 (1999).
- [9] A. M. Hlggins and R. A. L. Jones, Nature **404**, 476 (2000).
- [10] A. Karim *et al.*, Phys. Rev. E. **57**, R6273 (1998).
- [11] G. Lopez *et al.*, Science **260**, 647 (1993).
- [12] R. Konnur, K. Kargupta and A. Sharma, Phys. Rev. Lett. **84**, 931 (2000); K. Kargupta, R. Konnur and A. Sharma, Langmuir (in press).
- [13] G. Reiter, R. Khanna and A. Sharma, Phys. Rev. Lett. **85**, 1432 (2000); S. Herminghaus *et al.*, Science **282**, 916 (1998); A. Oron, Phys. Rev. Lett. **85**, 2108 (2000).
- [14] A. Sharma, R. Khanna, Phys. Rev. Lett. **81**, 3463 (1998).
- [15] U. Thiele, M. Mertig and W. Pompe, Phys. Rev. Lett. **80**, 2869 (1998); A. S. Padmakar, K. Kargupta and A. Sharma, J. Chem. Phys. **110**, 1735 (1999).
- [16] H. I. Kim *et al.*, Phys. Rev. Lett. **82**, 3496 (1999).

- [17] C. J. Van Oss, M. K. Chaudhury and R. J. Good, Chem. Rev. **88**, 927 (1988).